RESEARCH ARTICLE

A Visible-Light-Harvesting Covalent Organic Framework Bearing Single Nickel Sites as a Highly Efficient Sulfur-Carbon Cross-Coupling Dual Catalyst

Hui Chen,[a] Wanlu Liu,[a,b] Andreas Laemont,[a] Chidharth Krishnaraj,[a] Xiao Feng,[a] Fadli Rohman,[c] Maria Meledina,[c,d] Qiqi Zhang,[e] Rik Van Deun,[b] Karen Leus,[a] and Pascal Van Der Voort*[a]

[a] Prof. P. Van Der Voort, H. Chen, W.-L. Liu, A. Laemont, C. Krishnaraj, Dr. X. Feng, Dr. K. Leus
COMOC-Center for Ordered Materials, Organometallics and Catalysis.
Department of Chemistry, Ghent University.
Krijgslaan 281-S3, 9000 Ghent, Belgium
E-mail: Pascal.VanDerVoort@UGent.be

[b] Prof. R. Van Deun, W.-L. Liu,
L^3-Luminescent Lanthanide Lab.
Department of Chemistry, Ghent University.
Krijgslaan 281-S3, 9000 Ghent, Belgium.

[c] Dr. M. Meledina, F. Rohman
RWTH Aachen University.
Central Facility for Electron Microscopy.
D-52074, Aachen, Germany.

[d] Dr. M. Meledina,
Forschungszentrum Jülich GmbH.
Ernst Ruska-Centre (ER-C 2).
D-52425, Jülich, Germany.

[e] Q.-Q. Zhang,
TJU-NIMS International Collaboration Laboratory,
School of Materials Science and Engineering, Tianjin University.
No. 92 Weijin Road, Nankai District, Tianjin 300072, P. R. China.

Supporting information for this article is given via a link at the end of the document.

Abstract: Covalent-Organic-Frameworks (COFs) have recently emerged as light-harvesting devices, as well as elegant heterogeneous catalysts. The combination of these two properties into a dual catalyst has not been explored yet. Here, we report a new photosensitive triazine-based COF, decorated with single Ni-sites to form a dual catalyst. This crystalline and highly porous catalyst shows excellent catalytic performance in the visible-light-driven catalytic sulfur-carbon cross-coupling reaction. The ability to incorporate single transition metal sites in a photosensitive COF scaffold which acts as a two-component synergistic catalyst in organic transformation is demonstrated for the first time.

Introduction

Organosulfur compounds such as methionine, glutathione, biotin, *etc.* are widely present in various biological systems, and play a crucial role in vital processes of living organisms[1]. In addition to this, they are also often found in artificial synthetic drugs such as potential HIV inhibitors, esomeprazole, duloxetine hydrochloride, *etc.*[2]. Because of their broad applicability in biological processes and pharmaceuticals, the formation of sulfur-carbon bonds (S-C bonds) is of paramount importance in modern synthetic organic chemistry. Traditionally, S-C bonds are formed by transition metal-catalyzed cross-coupling reactions using copper, iron, palladium, nickel, *etc.* (**Scheme 1a**)[3]. Unfortunately, harsh synthesis conditions are typically required, such as the presence of strong bases and the need for high temperatures, which often leads to a low functional group tolerance. Also, highly specific and expensive ligands combined with high catalyst loadings are required as thiols are prone to dimerization and coordination to the transition-metals[4]. To overcome these shortcomings, visible-light-driven organic transformations have received attention as they allow an environmentally friendly and sustainable strategy to perform organic reactions in very mild conditions[5].

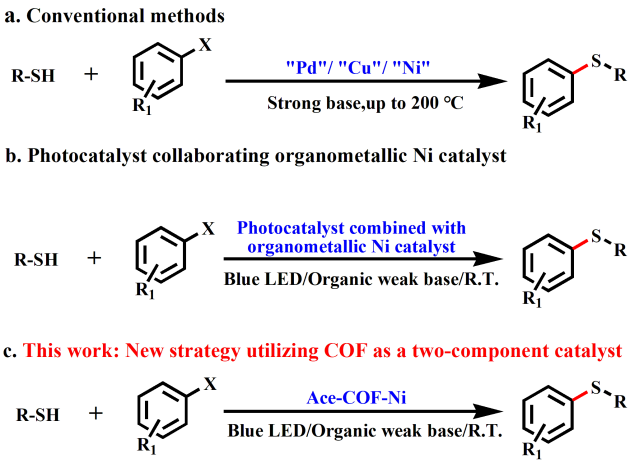

Scheme 1. Various methods for the formation of S-C bonds.

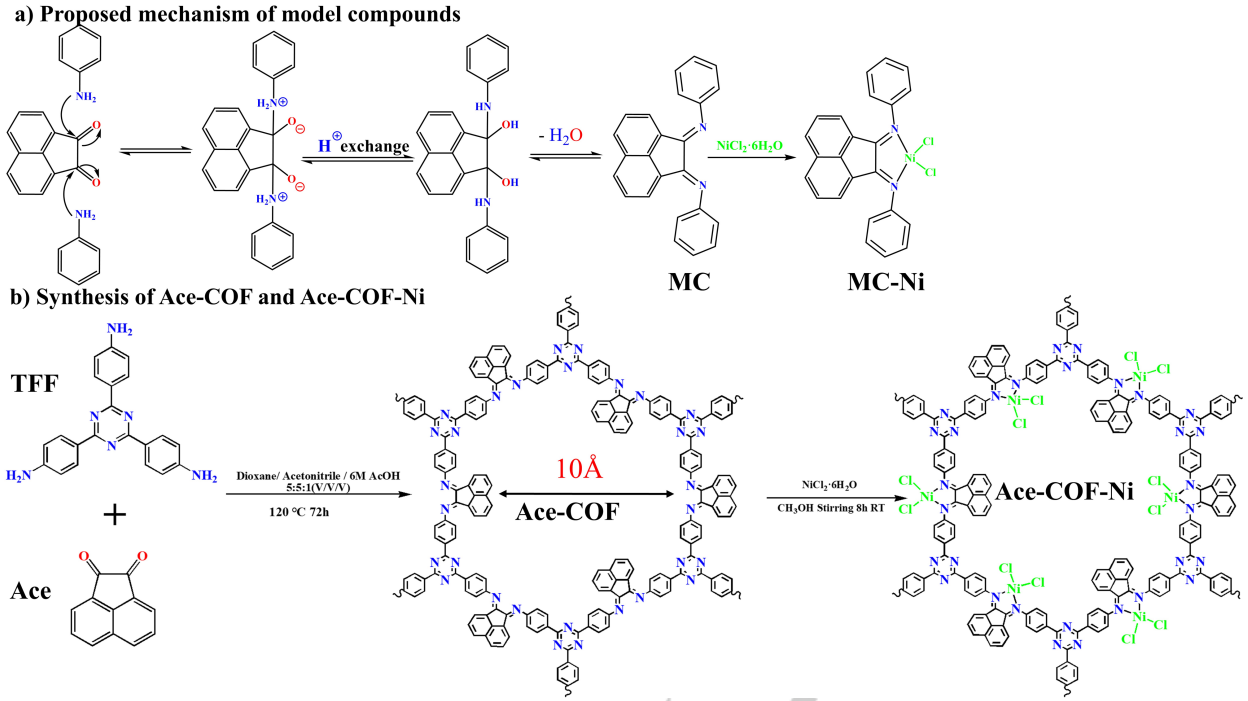

Scheme 2. The synthesis process of (a) model compound and (b) Ace-COF-Ni.

Within this context, several photosensitive molecules such as noble metal complexes ($Ir[dF(CF_3)ppy]_2(bpy)PF_6$, $Ru(bpy)_3]Cl_2$)[3d,6], organic dyes (Eosin Y)[7], and inorganic semiconductors (TiO_2, Bi_2O_3)[8] have been used as homogeneous photocatalysts for a variety of organic reactions through a single electron transfer (SET) mechanism. In 2016, Johannes and co-workers employed $Ir[dF(CF_3)ppy]_2(dtbbpy)PF_6$ as photocatalyst combined with an organometallic Ni catalyst exhibiting a synergistic effect in S-C cross-coupling reactions at room temperature[6]. Later on, Molander's group developed a photoredox/Nickel dual catalyst using $[Ru(bpy)_3](PF_6)_2$ in thioetherification[3d] (**Scheme 1b**). In both studies, the catalysts exhibited a high efficiency with yields of up to 95%. Nevertheless, the inherent disadvantages of homogeneous catalysts such as their low recyclability and high cost limit their industrial implementation. For this reason, there is an urgent need to develop heterogeneous visible-light-driven photocatalysts for the formation of S-C bonds that can be easily recycled without loss in activity and yield.

In 2005, Omar Yaghi reported for the first time the synthesis of a Covalent Organic Framework (COF) triggering the development of several new structures[9]. COFs are crystalline two or three-dimensional organic porous solids, constructed from organic building blocks that are linked by strong covalent bonds[10]. COFs have been widely recognized as potential heterogeneous photocatalysts due to their inherent light-harvesting and energy transition capabilities as a consequence of their remarkable features including large specific surface areas, π-π stacking interactions, long-range order, and hierarchically integrated building blocks[11]. However, so far, photosensitive COFs have mostly been employed in studying both half-reactions for water splitting and CO_2 reduction[12]. Only a minority of COFs have been studied to catalyze organic transformations[13], of which all of them were based on single components that served either as a photosensitizer or as solid support. The application of COFs in two-component or multi-component catalysis is up until now an unexplored field. Inspired by these promising developments on the use of COFs in photosynthesis, we hypothesized that COFs might form an ideal platform to combine photoredox and transition-metal catalysts to drive organic transformations. Herein, we report a novel triazine-based COF, which not only acts as a photocatalyst but also as a support material to incorporate nickel catalytic active sites. The ordered structure with high porosity and the proximity of the photosensitizing COF framework and the nickel catalytic active sites significantly improves the catalytic efficiency, as it facilitates the electron and thiol radical transfers from the photosensitizer to the Ni catalytic active sites.

Results and Discussion

Initially, the model compound (marked as MC) was synthesized to illustrate the possibility of acenaphthenequinone and amine condensation (**Scheme 2a**). The successful synthesis of MC is confirmed by ^1H NMR and matched with the literature report (**Figure S1**)[14]. Acenaphthenequinone was chosen because it easily condenses with amine groups, allowing the construction of robust, crystalline COF structures. Moreover, the resulting 1,2-Bis(phenylamino)-acenaphthene moiety can chelate transition metal ions for organometallic catalytic reactions[15]. Based on this, the photosensitive triazine-based COF scaffold (denoted as Ace-COF) was prepared under solvothermal conditions in a sealed ampule through the condensation of 4,4′ 4 ″ - (1,3,5-triazine-2,4,6-triyl)trianiline (TTA) and acenaphthenequinone (Ace). These two building blocks were selected because their planar structure ensures high π-π interactions between the layers to obtain a highly crystalline COF. Also, the use of these building blocks ensures the presence of

distinct electronic donor-acceptor structures that offer topologically ordered D-A heterojunctions with independent pathways for ambipolar electron and hole transport resulting in enhanced photoconductivity and photocatalytic activity[13a, 16]. After a thorough screening of several synthesis parameters including temperature, solvent, and reaction time (**Table S1, Figure S3**), it was observed that the optimal synthesis conditions were as follows: condensation of 0.1 mmol TTA (35.5 mg) and 0.15 mmol Ace (27.3 mg) in an acetonitrile/1,4-dioxane/6M aqueous acetic acid (1.1 mL, 5:5:1 by vol.) solvent mixture at a reaction temperature of 120 °C for 3 days. The Ace-COF exhibits remarkable chemical stability in common organic solvents, HCl (1 M) and NaOH (1 M) aqueous. After soaking the material in each of these media for 7 days, no change in the PXRD pattern was observed, which indicates that the crystallinity was preserved (**Figure S4**). Ni ions were introduced into the Ace-COF scaffold through a simple post-synthetic wet impregnation with $NiCl_2 \cdot 6H_2O$ (denoted as Ace-COF-Ni, **Scheme 2b**).

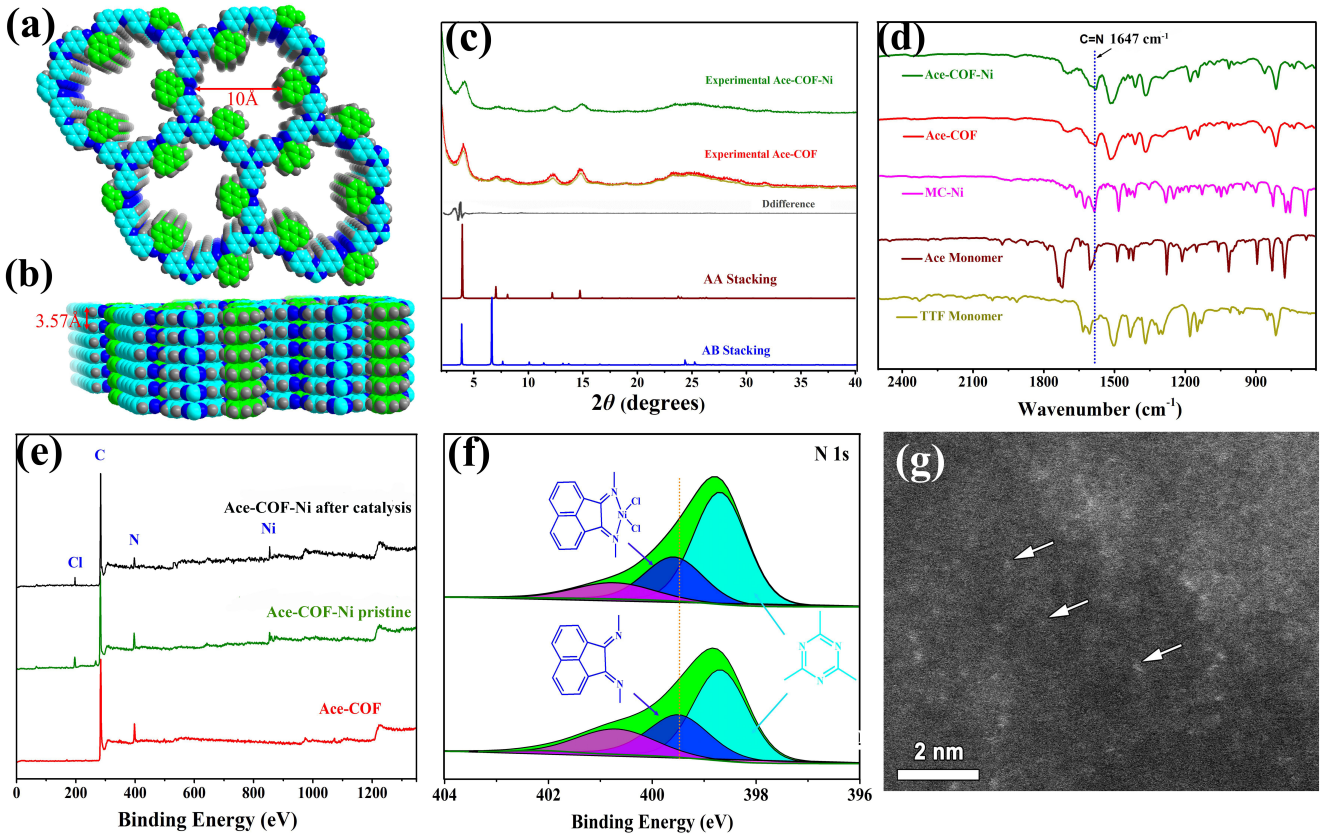

Figure 1. (a)Top and (b) side views of Ace-COF. (c) PXRD pattern of Experimental Ace-COF (red) and Ace-COF-Ni (olive), Pawley-refined (faint yellow), Difference (black), and the simulated PXRD pattern of Ace-COF AA eclipsed stacking (wine) and AB staggered stacking (blue). (d) FT-IR spectrum of Ace-COF and Ace-COF-Ni. (e) XPS spectra of Ace-COF and Ace-COF-Ni. (f) N 1s XPS spectra of Ace-COF and Ace-COF-Ni. (g) Z-contrast HAADF-STEM image of Ace-COF-Ni: bright contras features (some examples are labeled by the white arrows) correspond to single Ni sites within the COF support.

The crystalline structure of the Ace-COF and Ace-COF-Ni compounds was determined by means of powder X-ray diffraction (PXRD) analysis (**Figure 1c**). The relatively sharp diffraction peaks reveal the good crystallinity of the materials. The reflections at 4.0°, 7.1°, 8.0°, 12.1°, and 14.7° correspond to the (100), (110), (200), (210), and (120) facets, respectively, whereas the slightly broader peak at higher 2θ (~ 25°) originates from the π-π stacking between the COF layers and corresponds to the (001) plane. All the diffraction peaks follow the *P-6* space group that represents a hexagonal 2D layered network. The structural simulation of Ace-COF shows that an eclipsed AA stacking mode is preferred over a staggered AB stacking. Pawley refinements of the experimental PXRD profiles was carried out and the refinement results yield unit cell parameters are $\boldsymbol{a} = \boldsymbol{b} = 28.7668$ Å, $\boldsymbol{c} = 3.5734$ Å, and $\boldsymbol{\alpha} = \boldsymbol{\beta} = 90°$, $\boldsymbol{\gamma} = 120°$, which match well with the predictions with good agreement factors ($R_{wp} = 4.23\%$ and $R_p = 5.08\%$). The PXRD pattern of the Ace-COF-Ni is similar to that of the pure Ace-COF (**Figure 1c**), indicating that the crystalline structure of the COF is retained upon the introduction of the Ni ions.

The Fourier transform infrared (FT-IR) spectra of the Ace-COF-Ni and pristine Ace-COF (**Figure 1d**) exhibit a typical vibration band at 1647 cm^{-1} which confirms the successful formation of the imine bond (C=N). Further structural information on the coordination of the Ni ions in the Ace-COF was obtained employing X-ray photoelectron spectroscopy (XPS). The XPS spectrum of Ace-COF-Ni shows the presence of Cl, C, N, and Ni (**Figure 1e**). The binding energy of the Ni 2p peak at 856 eV can be assigned to Ni^{2+} (**Figure S5**). This value is similar to the reported value for $NiCl_2 \cdot$bpy (bpy = 2,2'-bipyridine)[12c], which indicates the successful coordination of Ni ions with the framework. No signals were found for any other Ni species, such as NiO and metallic Ni. Moreover, a slight shift of the N 1s peaks

to higher binding energy was observed in the Ace-COF-Ni material in comparison to the N 1s XPS spectrum of the pristine Ace-COF (**Figure 1f**). This shift can be ascribed to the coordination of the nitrogen atoms to Ni^{2+} and is consistent with literature reports [12c]. Scanning electron microscopy (SEM) analyses show spherical morphologies of Ace-COF-Ni (**Figure S6**). In the high-resolution transmission electron microscopy (HR-TEM) images, no Ni nanoparticles were observed (**Figure S7**). The energy-dispersive X-ray (EDX) mapping images of the Ace-COF-Ni give clear evidence for the presence of C, N, Cl, and Ni which are homogeneously distributed in the COF matrix (**Figure S7 and S8**). Bright contrast features in the Z-contrast HAADF-STEM image correspond to single atoms spread within the Ace-COF supporting material (**Figure 1g**), some examples are marked by the white arrows). Ni as the heaviest element in the Ace-COF-Ni, the bright contrast features highlighted by the white arrows in the Z-contrast HAADF-STEM images can be safely attributed to single sites of Ni sitting within the Ace-COF network. The Ni content, determined by inductively coupled plasma mass spectrometry (ICP-MS) is 1.03 mmol/g.

The surface area of the Ace-COF and Ace-COF-Ni compound was determined by measuring the Argon adsorption isotherm at 87 K of the activated samples. As shown in **Figure S9a**, a sharp increase in the gas uptake is observed at low relative pressures ($P/P_0 < 0.1$) indicating the presence of micropores. The Brunauer-Emmett-Teller (BET) surface area and total pore volume (at P/P_0=0.97) decreased from 1238 $m^2 g^{-1}$ and 0.85 $cm^3 g^{-1}$ for Ace-COF to 825 $m^2 g^{-1}$ and 0.61 $cm^3 g^{-1}$ for Ace-COF-Ni, respectively. The pore sizes of both the Ace-COF and Ace-COF-Ni were calculated to be 0.97 nm in diameter using Ar at 87K quenched solid density functional theory (QSDFT) carbon model (**Figure S9b**). From these observations, it is clear that, although the interior cavities of the Ace-COF-Ni are partially occupied by Ni ions, the Ace-COF-Ni structure exhibits a permanent open structure, ensuring a good diffusion of the reactants to the Ni active sites. Besides a permanent porosity, thermal stability is also very important for its practical application as a heterogeneous catalyst. As indicated in **Figure S10**, the thermogravimetric analysis (TGA) shows that both Ace-COF and Ace-COF-Ni possess excellent thermal stability, up to 450 °C under a nitrogen atmosphere.

The optical properties of Ace-COF-Ni and Ace-COF were assessed to verify the feasibility of using Ace-COF-Ni to catalyze reactions under visible light irradiation solely. UV-Vis absorption experiments are carried out at room temperature, the UV-vis spectra indicate that the Ace-COF and the Ace-COF-Ni can absorb light in the UV and visible regions (**Figure S11**). However, the Ace-COF-Ni model compound (abbreviated as MC-Ni, **Scheme 2a**) only absorbs UV light. The optical bandgaps of Ace-COF, Ace-COF-Ni, and MC-Ni were analyzed to be 1.74 eV, 1.83 eV, and 2.85 eV, respectively. Ace-COF and Ace-COF-Ni have a much smaller bandgap than the model compound, this can be explained by the introduction of the electron-accepting triazine unit, the extended imine conjugation in the x and y direction of the COF structure, and enhanced π-conjugation between the COF layers. In comparison with the previously reported photocatalytic COFs, such as LZU-190, LZU-191, and LZU-192 (optical band gaps are 2.02 eV, 2.38 eV, and 2.10 eV, respectively)[13b]. Ace-COF-Ni and Ace-COF show enhanced absorption in the visible light range. This implies that the Ace-COF-Ni is a promising platform for visible-light-driven organic transformation reactions.

Table 1. Ace-COF-Ni dual-catalyzed S-C cross-coupling: influence of reaction

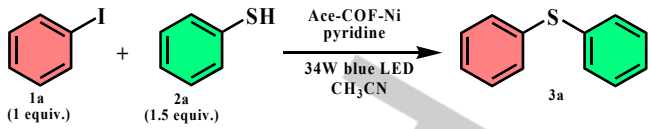

parameters.

Entry	Variation from the standard conditions	Yield (%)[b]
1	Standard conditions[a]	>95
2	No light (dark)	No Product
3	No pyridine	No Product
4	No Ace-COF-Ni	No Product
5	MC-Ni instead of Ace-COF-Ni	No Product
6	Ace-COF instead of Ace-COF-Ni	No Product
7	Ace-COF mixed $NiCl_2{\cdot}6H_2O$ instead of Ace-COF-Ni	58
8	Ace-COF mixed MC-Ni instead of Ace-COF-Ni	26
9	0.5 mol % Ace-COF-Ni	35
10	1 mol % Ace-COF-Ni	73
11	2 mol % Ace-COF-Ni	>95

[a] Standard conditions: Under an Ar atmosphere, 0.50 mmol 1a, 0.75 mmol 2a, 2 mol % Ace-COF-Ni, pyridine 1 mmol, and 5 mL of 99.8% anhydrous acetonitrile, then 34W blue LED irradiation for 24h at R.T. [b] yield was determined by ^1H NMR with CH_3NO_2 as an internal standard.

Therefore, the Ace-COF-Ni was examined in the visible-light-driven S-C cross-coupling reaction to evaluate its potential as a dual catalyst. First, iodobenzene (**1a**) and thiophenol (**2a**) were used as model substrates for the optimization of the reaction conditions (**Table 1**). More specifically, under an Ar atmosphere, a reaction mixture of iodobenzene (0.5 mmol) (**1a**), thiophenol (0.75 mmol) (**2a**), 2 mol% Ace-COF-Ni, and pyridine (1 mmol) in anhydrous acetonitrile (5 ml) was irradiated with 34W blue LEDs (420 - 430 nm). After 24 hours, an excellent yield (> 95%) towards the corresponding S-C cross-coupled product phenyl sulfide (**3a**) was obtained at room temperature (**Table 1, entry 1**). From the blank tests, it was noted that no reaction occurred in the absence of light, the absence of pyridine, or the absence of Ace-COF-Ni (**Table 1, Entry 2, 3, and 4**). When the model compound MC-Ni instead of the Ace-COF-Ni was added into the reaction mixture, no detectable product of phenyl sulfide was observed, which suggests that the photosensitive triazine-based Ace-COF scaffold is essential (**Table 1, Entry 5**). When using Ace-COF instead of Ace-COF-Ni, no product was detected, implying that Ni also plays a crucial role in this cross-coupling reaction (**Table 1, Entry 6**). Interestingly, when using a physical mixture of either Ace-COF and $NiCl_2{\cdot}6H_2O$ or Ace-COF and the model compound MC-Ni as the catalyst (**Table 1, Entry 7 and 8**), also significant amounts of the product was observed (58%, 26%), albeit much lower than with the Ace-COF-Ni. This might be due to the *in-situ* formation of Ace-COF-Ni by Ace-COF scaffold and $NiCl_2{\cdot}6H_2O$. In the case of the mixture of MC-Ni and Ace-COF, the COF will act as the required photosensitizer to allow the reaction to proceed, which has been reported previously[17]. Based on these results, it is clear that both photosensitive triazine-based Ace-COF scaffold and Ni are required to perform the S-C cross-coupling reaction. A significant increase in the yield was observed upon increasing the amount of catalyst. When the amount of catalyst was increased from 0.5 to 1 and 2 mol %, the yield increased from 35 to 73 and 95%, respectively (**Table 1, Entry 9, 10, and 11**). This observation further corroborates the key role of the Ace-COF-Ni catalyst for this model reaction. A screening of several solvents (**Table S3**) showed that polar solvents (DMF, CH_3OH, DMSO, *etc.*) are more beneficial for the reaction whereas nonpolar solvents (toluene, hexane, *etc.*) showed a negative influence on

the reaction thermodynamic or/and kinetic control. This may be explained by the Hughes–Ingold rules[18], that state that polar solvents enhance the production of polar compounds. This is definitely the case for the photocatalytic S-C cross-coupling reaction, as many intermediates are polar, ionic, or radical. Hence, anhydrous acetonitrile was chosen as the optimum solvent for further reactions.

Table 2: Substrate scope of Ace-COF-Ni catalyzed cross-coupling between aryl iodides and thiols.

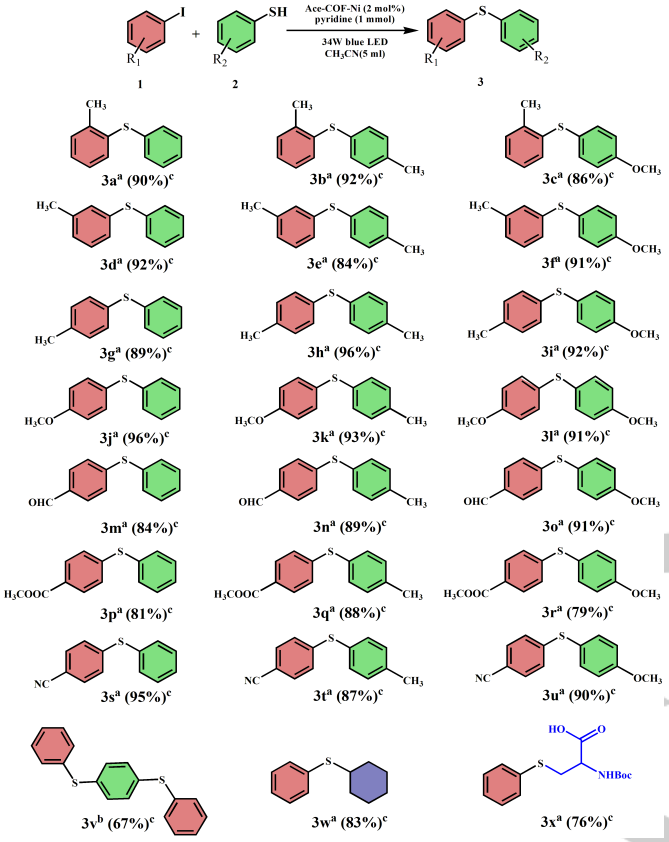

[a] Under Ar atmosphere, 0.50 mmol **1**, 0.75 mmol **2**, 2 mol % Ace-COF-Ni, 1 mmol pyridine, and 5 mL of anhydrous CH_3CN, blue LED irradiation for 24h at R.T., [b] 1 mmol of iodobenzene. [c] % yield was determined by ^1H NMR with CH_3NO_2 as an internal standard.

In a final stage, the scope of substrates was extended to examine the wide applicability of the Ace-COF-Ni catalyst in S-C cross-coupling reactions. Diverse aryl iodides containing either electron-withdrawing or electron-donating groups, such as methyl, methoxy, formyl, carbomethoxy, or cyano groups, and three different aryl thiols bearing hydrogen, methyl, or methoxy groups were chosen as substrates. The reactions were performed under the optimized reaction conditions in the presence of 2 mol% Ace-COF-Ni (**Table 2**). For each S-C cross-coupling reaction, an excellent yield (79 - 96 %) of the corresponding coupling product was obtained. When comparing **3a**, **3d**, and **3g**, it is noted that there is no significant influence of the position of the substituent on the resulting yield. Also, for substrates that possess electron-neutral or electron-rich substituents, a satisfactory yield was obtained (**3j**, **3m**, and **3p**). In addition to this, not only aryl thiols but also alkyl thiols gave the desired thioethers in good yield (**3w** and **3x**). From these observations, it can be concluded that the Ace-COF-Ni catalyst can be used to convert a wide range of substrates and that there is no significant influence of the functional groups on the resulting activity. Another important aspect of its practical implementation is the recyclability of the catalyst. The model substrates (**Table 1, entry 1**) were chosen to evaluate the recyclability of the Ace-COF-Ni catalyst. As can be seen from **Figure 2a**, the catalyst could be recovered and reused for at least five cycles without loss of catalytic performance. After five cycles of catalysis, no Ni leaching was detected by ICP-MS. The XPS spectrum of Ace-COF-Ni shows that the Ni 2p peak at 855 eV is not changed (**Figure S5**) and the Far-infrared spectra indicate the presence of the Ni-Cl bond[19] (**Figure S12**). Also, no apparent change in the PXRD patterns of the Ace-COF-Ni material. All this evidence indicating that the structure of Ace-COF-Ni was preserved (**Figure S13**).

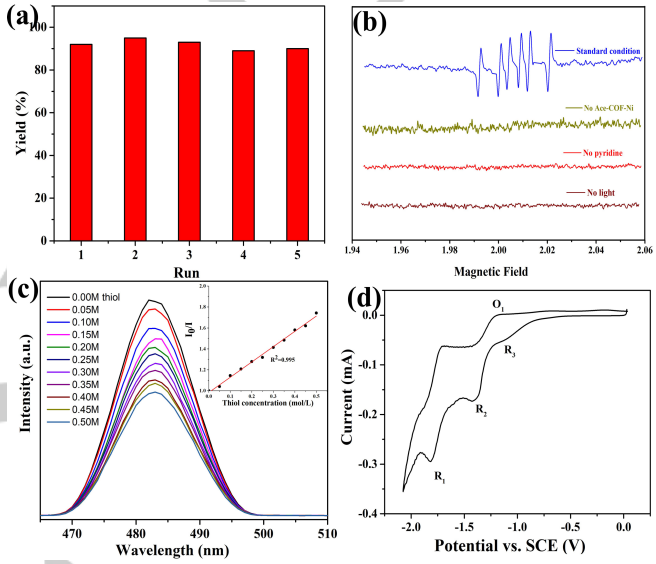

Figure 2. (a) Assessment of the reusability of Ace-COF-Ni, the reusability tests were carried out under identical conditions as shown in Table 1, entry 1. (b) The EPR spectroscopy under various conditions. The standard conditions are the same as Table 1, entry 1. (c) Steady-state emission quenching of Ace-COF-Ni* with thiol; (Inset) Stern-Volmer analysis of the results. (d) The CV curve of the Ace-COF-Ni model compound MC-Ni versus SCE in CH_3CN in the presence of 0.1 M pyridine.

In order to obtain insights into the reaction mechanism, photophysical and electrochemical measurements were performed. In the first instance, to determine whether there is an electron transfer between the excited state of Ace-COF-Ni (marked as Ace-COF-Ni*) and the thiophenol or the aryl iodide, steady-state emission quenching of Ace-COF-Ni* with varying thiol and aryl iodide concentration was performed. From this experiment, it was observed that an increase in the concentration of thiophenol and aryl iodide resulted in a weaker fluorescence intensity for which the Stern-Volmer analysis exhibited an excellent linear regression (**Figure 2c, Figure S14**). The quenching efficiencies for thiophenol and aryl iodide were quantified by the Stern–Volmer equation: $(I_0/I) = 1 + k_{sv}[Q]$, resulting in a quenching constant k_{sv} for thiophenol and aryl iodide of 1.459±0.005 M^{-1} and 0.282±0.008 M^{-1}, respectively. The thiophenol is thus almost five times more effective than the aryl iodide in quenching the Ace-COF-Ni* luminescence. This might be because the aryl iodide quenches the Ace-COF-Ni* luminescence by energy transfer rather than electron transfer[20]. Moreover, time-resolved emission spectroscopy shows that the lifetime of the Ace-COF-Ni* is ~5 μs as determined by its emission

at 485 nm. Interestingly, upon the addition of the thiophenol, the excited state lifetime is significantly decayed. More specifically, when the thiol concentration amounts to 0.5 M, the excited state lifetime of Ace-COF-Ni* is only ~3.5 μs (**Figure S15**). In conclusion, the combined time-resolved emission spectroscopy and steady-state emission quenching experiments indicate that the initial step in the photocatalytic process involves the reductive quenching of Ace-COF-Ni* by thiophenol to generate the thiophenol radical.

Furthermore, we investigated the types of radicals produced during the reaction by electron paramagnetic resonance (EPR) spectroscopy. Under an Ar atmosphere, a mixture of 0.5 mmol thiophenol (**2a**), 2 mol % Ace-COF-Ni, 1 mmol pyridine, 5 mL anhydrous CH_3CN, and 5,5-dimethyl-1-pyrroline N-oxide (DMPO) as a radical trap was stirred for 20 minutes in the dark. Hereafter, a small amount of the mixture was transferred into a capillary. The EPR spectra of this mixture were recorded under different conditions. As shown in **Figure 2b**, no radical signal was observed without light irradiation, Ace-COF-Ni, or Pyridine. But, a sextet signal with a g = 2.006 (AN=1.33 mT, AH=1.47 mT) was observed under light irradiation, indicating that a sulfur-centered radical was produced[21]. It further confirms the conclusion of the time-resolved emission spectroscopy and steady-state emission quenching experiments that a reductive quenching of Ace-COF-Ni* by thiophenol occurs to generate the thiophenol radical.

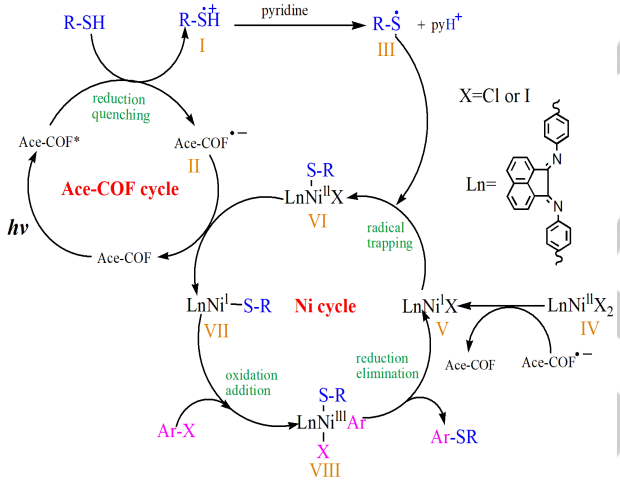

Scheme 3. Proposed mechanism of Ace-COF-Ni catalyzed S-C cross-coupling reaction.

To rationalize the dependence of the oxidation state of Ni in the cross-coupling reaction, electrochemical studies on the Ace-COF-Ni model compound MC-Ni in MeCN were performed. **Figure S16** shows the cyclic voltammetry (CV) curve of MC-Ni with two distinct reduction peaks at -1.81 V ($\mathbf{R_1}$) and -1.44 V ($\mathbf{R_2}$), versus a saturated calomel electrode (SCE) in MeCN, which correspond to the $Ni^0/Ni^{0\bullet-}$ and Ni^{II}/Ni^0 couples, respectively[22]. However, when pyridine is present, a new reduction peak $\mathbf{R_3}$ at -0.98 V and a new oxidation peak $\mathbf{O_1}$ at -1.08 V is observed besides the reduction peaks $\mathbf{R_1}$ and $\mathbf{R_2}$, which can be ascribed to a pyridine stabilized Ni^I-species[22a, 23] (**Figure 2d**). As the Ni^{II}/Ni^0 couple reduction potentials of MC-Ni are very close to the reduction potential of the triazine-based COF (-1.5 V versus SCE)[13a]. It is rather difficult to accurately ascertain the thermodynamic preference towards reduction to Ni^0. Nevertheless, as the reduction potential of the triazine-based COF is more negative than the Ni^I-species, this indicates that the triazine-based COF can easily reduce Ni^{II} to Ni^I. This result supports that the Ni^I-species are the thermodynamically and kinetically active species in the catalytic cycle.

Based on the obtained photophysical and electrochemical analyses described above, we propose the following mechanism for the visible-light-driven dual-catalytic S-C cross-coupling reaction (see **Scheme 3**). In this dual-catalytic process, the Ace-COF cycle and Ni cycle are connected to each other through both electron and radical transfers. Upon visible-light irradiation, the photosensitive Ace-COF-Ni generates an excited state Ace-COF-Ni*. This is followed by a single electron transfer (SET) oxidation of the thiol through the photoexcited Ace-COF-Ni*, which produces both the thiol radical cation (**I**) and the Ace-COF-$Ni^{\bullet-}$ (**II**) complex. In the presence of pyridine, the thiol radical cation (**I**) is deprotonated and converted to the thiol radical (**III**). A SET reduction of the Ace-COF-Ni by Ace-COF-$Ni^{\bullet-}$ (**II**) delivers a Ni^I-halide (**V**) while at the same time the Ace-COF-Ni is regenerated. The thiol radical (**III**) then rapidly combines with the Ni^I-halide (**V**) to form a Ni^{II}-sulfide complex (**VI**). This Ni^{II}-sulfide complex (**VI**) is then again reduced to a Ni^I-sulfide complex (**VII**) by Ace-COF-$Ni^{\bullet-}$, which in the following step undergoes an oxidative addition of the aryl iodide to produce a Ni^{III}-complex. Through a facile reductive elimination process, the targeted S-C cross-coupled product is formed and a Ni^I-halide (**V**) is released. Oderine *et al.* found a similar electron transfer when studying the homogeneous $Ir[dF(CF_3)ppy]_2(dtbbpy)PF_6$ combined with organometallic Ni catalyst for the same cross-coupling reaction[6].

Conclusion

In summary, we have developed a novel imine-linked triazine-based COF dual catalyst. The photoactive COF acts as the photocatalyst while the incorporated single nickel sites act as the active transition metal species for the visible-light-driven S-C cross-coupling reaction. The resulting Ace-COF-Ni exhibits high catalytic activity, broad substrate adaptability, and outstanding recyclability and stability due to the ordered structure and proximity of the photosensitizer and the nickel catalytic active sites. This work demonstrates, for the first time, the ability to incorporate transition metal single sites in a photosensitive Ace-COF scaffold and to form a dual catalyst to synergistically perform organic transformations.

Acknowledgements

We thank Prof. Dirk Poelman (UGent) for helping with the Solid-state UV-vis measurements and thank Prof. Henk Vrielinck (UGent) for Far-infrared spectral measurements. H.C. and W.L.L. gratefully acknowledge the Chinese Scholarship Council (CSC) for financial support. M. M. gratefully acknowledges the Verbundvorhaben iNEW: Inkubator Nachhaltige Elektrochemische Wertschöpfungsketten with the funding number 03SF0589A for financial support. C.K. and P.V.D.V acknowledges the support from the Research Board of Ghent University (GOA010-17, BOF GOA2017000303). A.L. acknowledges the financial support from the Ghent University

BOF doctoral grant 01D12819. K.L. thanks the financial support from Ghent University.

Keywords: Covalent Organic Framework • Single Nickel Sites • visible-light-driven photocatalyst • dual catalyst • Sulfur-Carbon Cross-Coupling reaction

[1] J. F. Da Silva, R. J. P. Williams in *The biological chemistry of the elements: the inorganic chemistry of life*, Oxford University Press, **2001**.

[2] a) L. A. Damani in *Sulphur containing drugs and related organic compounds: chemistry, biochemistry, and toxicology, Vol. 3*, Ellis Horwood, **1989**; b) A. Nudelman in *Chemistry of optically active sulfur compounds*, **1984**.

[3] a) X. Wang, G. D. Cuny, T. Noël, *Angew. Chem. Int. Ed.* **2013**, 52, 7860-7864; b) X. Moreau, J.-M. Campagne, *J. Org. Chem.* **2003**, 68, 5346-5350; c) A. Correa, M. Carril, C. Bolm, *Angew. Chem. Int. Ed.* **2008**, 47, 2880-2883; d) M. Jouffroy, C. B. Kelly, G. A. Molander, *Org. Lett.* **2016**, 18, 876-879.

[4] a) P. Chauhan, S. Mahajan, D. Enders, *Chem. Rev.* **2014**, 114, 8807-8864; b) R. B. Othman, S. Massip, M. Marchivie, C. Jarry, J. Vercouillie, S. Chalon, G. Guillaumet, F. Suzenet, S. Routier, *Eur. J. Org. Chem.* **2014**, 3225-3231; c) A. Wimmer, B. Konig, Beilstein *J. Org. Chem.* **2018**, 14, 54-83.

[5] a) X. Lang, X. Chen, J. Zhao, *Chem. Soc. Rev.* **2014**, 43, 473-486; b) Q. Liu, L.-Z. Wu, *Natl. Sci. Rev.* **2017**, 4, 359-380; c) K. T. Ngo, J. Rochford, in *Green Chemistry*, Elsevier, **2018**, pp. 729-752.

[6] M. S. Oderinde, M. Frenette, D. W. Robbins, B. Aquila, J. W. Johannes, *J. Am. Chem. Soc.* **2016**, 138, 1760-1763.

[7] X. Z. Fan, J. W. Rong, H. L. Wu, Q. Zhou, H. P. Deng, J. D. Tan, C. W. Xue, L. Z. Wu, H. R. Tao, J. Wu, *Angew. Chem. Int. Ed.* **2018**, 57, 8514-8518.

[8] a) K. Hashimoto, H. Irie, A. Fujishima, *Jpn. J. Appl. Phys.* **2005**, 44, 8269; b) Y. Dong, A. Ma, D. Zhang, Y. Gao, H. Li, *Surf. Innov.* **2020**, 1-8.

[9] a) A. P. Cote, A. I. Benin, N. W. Ockwig, M. O'Keeffe, A. J. Matzger, O. M. Yaghi, *science* **2005**, 310, 1166-1170; b) Wang L, Zeng C, Xu H, Yin P, Chen D, Deng J, Li M, Zheng N, Gu C, Ma Y. *Chemical science*. **2019**, 10(4), 1023-8; c) Su, Y., Wan, Y., Xu, H., Otake, K.I., Tang, X., Huang, L., Kitagawa, S. and Gu, C., *J. Am. Chem. Soc.* ***2020**, 142, 13316−13321*

[10] a) N. Huang, P. Wang, D. Jiang, *Nat. Rev. Mater.* **2016**, 1, 1-19; b) M. S. Lohse, T. Bein, *Adv. Funct. Mater.* **2018**, 28, 1705553; c) S. J. Lyle, P. J. Waller, O. M. Yaghi, *Trends in Chemistry*, May 2019, Vol. 1, No. 2, **2019**; d) X. Guan, F. Chen, Q. Fang, S. Qiu, *Chem. Soc. Rev.* **2020**, 49, 1357-1384.

[11] a) E. Jin, Z. Lan, Q. Jiang, K. Geng, G. Li, X. Wang, D. Jiang, *Chem.* **2019**, 5, 1632-1647; b) X. Kang, X. Wu, X. Han, C. Yuan, Y. Liu, Y. Cui, *Chem. Sci.* **2020**, 11, 1494-1502; c) X. Wang, L. Chen, S. Y. Chong, M. A. Little, Y. Wu, W.-H. Zhu, R. Clowes, Y. Yan, M. A. Zwijnenburg, R. S. Sprick, *Nat. Chem.* **2018**, 10, 1180-1189; d) S. Yang, W. Hu, X. Zhang, P. He, B. Pattengale, C. Liu, M. Cendejas, I. Hermans, X. Zhang, J. Zhang, *J. Am. Chem. Soc.* **2018**, 140, 14614-14618; e) f)

[12] a) T. Banerjee, K. Gottschling, G. Savasci, C. Ochsenfeld, B. V. Lotsch, *ACS Energy Lett.* **2018**, 3, 400-409; b) L. J. Wang, R. L. Wang, X. Zhang, J. L. Mu, Z. Y. Zhou, Z. M. Su, *ChemSusChem* **2020**, 13, 2973-2980; c) W. Zhong, R. Sa, L. Li, Y. He, L. Li, J. Bi, Z. Zhuang, Y. Yu, Z. Zou, *J. Am. Chem. Soc.* **2019**, 141, 7615-7621.

[13] a) Y. Zhi, Z. Li, X. Feng, H. Xia, Y. Zhang, Z. Shi, Y. Mu, X. Liu, *J. Mater. Chem. A* **2017**, 5, 22933-22938; b) P. F. Wei, M. Z. Qi, Z. P. Wang, S. Y. Ding, W. Yu, Q. Liu, L. K. Wang, H. Z. Wang, W. K. An, W. Wang, *J. Am. Chem. Soc.* **2018**, 140, 4623-4631.

[14] C. D. Nunes, P. D. Vaz, V. Felix, L. F. Veiros, T. Moniz, M. Rangel, S. Realista, A. C. Mourato, M. J. Calhorda, *Dalton. Trans.* **2015**, 44, 5125-5138.

[15] El Ashry, E.S.H., Hamid, H.A., Kassem, A.A. and Shoukry, M., *Molecules*, 2002. 7(2), pp.155-188.

[16] W. Chen, Z. Yang, Z. Xie, Y. Li, X. Yu, F. Lu, L. Chen, *J. Mater. Chem. A* **2019**, 7, 998-1004.

[17] X. Han, Q. Xia, J. Huang, Y. Liu, C. Tan, and Y. Cui, *J. Am. Chem. Soc.* **2017**, 139, 8693−8697.

[18] a) R. Kopelman, *Science*, **1988**, 1620-1626; b) B. Phyllis, F. Hiron, E. D. Hughes, C. K. Ingold, and P. A. D. S. Rao. *Nature* **1950**, no. 4213, 179-180.

[19] H. Irving and R. J. P. Williams, *J. Chem. Soc.*, **1953**, 3192.

[20] Y. Y. Zhu, G. Lan, Y. Fan, S. S. Veroneau, Y. Song, D. Micheroni, W. Lin, *Angew. Chem. Int. Ed.* **2018**, 57, 14090-14094.

[21] M. J. Davies, L. G. Forni, S. L. Shuter, *Chem.-Biol. Interact.* **1987**, 61, 177 – 188.

[22] a) C. Amatore, A. Jutand, *Organometallics* **1988**, 7, 2203-2214; b) P. Zhao, Y. W. Luo, T. Xue, A. J. Zhang, J. X. Lu, *Chin. J. Chem.* **2006**, 24, 877-880.

[23] C. Amatore, F. Gaubert, A. Jutand, J. H. P. Utley, *J. Chem. Soc., Perkin Trans. 2*, **1996**, 2447-2452

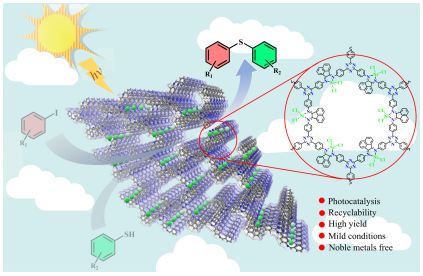

A dual catalyst (Ace-COF-Ni), which is composed of a photosensitive covalent organic framework and single nickel sites, is reported. This dual catalyst exhibits excellent visible-light and organometallic nickel synergistic catalytic performances for the Sulfur-Carbon Cross-Coupling reaction.